Journal of Molecular and Cellular Cardiology 74 (2014) 151–161

Contents lists available at ScienceDirect

Journal of Molecular and Cellular Cardiology

journal homepage: www.elsevier.com/locate/yjmcc

Functional improvement and maturation of rat and human engineered heart tissue by chronic electrical stimulation

Marc N. Hirt [a,b,1], Jasper Boeddinghaus [a,b,1], Alice Mitchell [c], Sebastian Schaaf [a], Christian Börnchen [d], Christian Müller [b,e], Herbert Schulz [f,g], Norbert Hubner [f,g], Justus Stenzig [a,b], Andrea Stoehr [a], Christiane Neuber [a,b], Alexandra Eder [a,b], Pradeep K. Luther [c], Arne Hansen [a,b,2], Thomas Eschenhagen [a,b,*,2]

[a] Department of Experimental Pharmacology and Toxicology, University Medical Center Hamburg-Eppendorf, Hamburg, Germany
[b] DZHK (German Centre for Cardiovascular Research), Partner Site Hamburg/Kiel/Lübeck, Germany
[c] Faculty of Medicine, National Heart & Lung Institute, Imperial College London, United Kingdom
[d] Dermatology and Venereology Department and Clinic, University Medical Center Hamburg-Eppendorf, Hamburg, Germany
[e] Department of General and Interventional Cardiology, University Medical Center Hamburg-Eppendorf, Hamburg, Germany
[f] Max-Delbruck-Center for Molecular Medicine (MDC), Berlin, Germany
[g] DZHK (German Centre for Cardiovascular Research), Partner Site Berlin, Germany

ARTICLE INFO

Article history:
Received 6 March 2014
Received in revised form 9 May 2014
Accepted 11 May 2014
Available online 19 May 2014

Keywords:
Electrical stimulation
Cardiac tissue engineering
Cardiomyocyte maturation
Induced pluripotent stem cells
Cardiomyocytes
2-photon microscopy

ABSTRACT

Spontaneously beating engineered heart tissue (EHT) represents an advanced in vitro model for drug testing and disease modeling, but cardiomyocytes in EHTs are less mature and generate lower forces than in the adult heart. We devised a novel pacing system integrated in a setup for videooptical recording of EHT contractile function over time and investigated whether sustained electrical field stimulation improved EHT properties. EHTs were generated from neonatal rat heart cells (rEHT, n = 96) or human induced pluripotent stem cell (hiPSC)-derived cardiomyocytes (hEHT, n = 19). Pacing with biphasic pulses was initiated on day 4 of culture. REHT continuously paced for 16–18 days at 0.5 Hz developed 2.2× higher forces than nonstimulated rEHT. This was reflected by higher cardiomyocyte density in the center of EHTs, increased connexin-43 abundance as investigated by two-photon microscopy and remarkably improved sarcomere ultrastructure including regular M-bands. Further signs of tissue maturation include a rightward shift (to more physiological values) of the Ca^{2+}-response curve, increased force response to isoprenaline and decreased spontaneous beating activity. Human EHTs stimulated at 2 Hz in the first week and 1.5 Hz thereafter developed 1.5× higher forces than nonstimulated hEHT on day 14, an ameliorated muscular network of longitudinally oriented cardiomyocytes and a higher cytoplasm-to-nucleus ratio. Taken together, continuous pacing improved structural and functional properties of rEHTs and hEHTs to an unprecedented level. Electrical stimulation appears to be an important step toward the generation of fully mature EHT.

1. Introduction

Cardiac tissue engineering aims at providing advanced in vitro models for drug testing and disease modeling as well as heart muscle tissue for cardiac regeneration [1]. With the recent progress in human pluripotent stem cell (hPSC) technologies and the principally unlimited availability of hPSC-derived cardiomyocytes, 3D human engineered heart tissues (hEHTs) will soon be widely available. Even so rodent EHTs are easier to produce, generally develop higher contractile force and are considerably cheaper than human EHT. They therefore still represent the workhorse in most laboratories. The 3D culture form of EHTs combined with directed mechanical load allows cardiomyocytes in EHTs to reach a higher degree of differentiation and maturation than standard 2D cultures [2], probably reaching the highest level possible

Abbreviations: cp-p, continuously paced group-paced state; cp-s, continuously paced group-spontaneous state; EC_{50}, half maximal effective concentration; ECM, extracellular Matrix; EHT, engineered heart tissue; FC, fold change; FS, fractional shortening; hEHT, human engineered heart tissue; hiPSC, human induced pluripotent stem cell; hPSC, human pluripotent stem cell; MLC2v, myosin regulatory light chain 2, ventricular isoform; rEHT, rat engineered heart tissue.

* Corresponding author at: Department of Experimental Pharmacology and Toxicology, University Medical Center Hamburg-Eppendorf, Martinistraße 52, 20246 Hamburg, Germany. Tel.: +49 40 7410 52180; fax: +49 40 7410 54876.
E-mail address: t.eschenhagen@uke.de (T. Eschenhagen).

[1] Both authors contributed equally to this work.
[2] Joint senior authors.

http://dx.doi.org/10.1016/j.yjmcc.2014.05.009

to date. However, both rodent [3] and human EHTs [4] and related 3D engineered cardiac constructs [5,6] show signs of cardiomyocyte immaturity. Differences compared to adult cardiomyocytes include the following. (i) Adult ventricular cardiomyocytes are quiescent and need a stimulus to beat [7]. Hence, spontaneous beating of EHTs from neonatal rodent cardiomyocytes or differentiated human pluripotent stem cells argues for immaturity. (ii) Twitch forces of freshly isolated human cardiomyocytes reach >50 mN/mm^2 [8], while regularly sized rodent EHTs rarely develop more than 1 mN/mm^2 (very thin ones reach >5 mN/mm^2) and human EHTs are frequently even weaker [9] although the group of Bursac recently reported considerably higher forces [10]. Part of this difference is due to a much lower volume fraction occupied by cardiomyocytes (compared to cell-free matrix) [11]. (iii) EHTs display hypersensitivity toward external calcium with an EC_{50} of 0.15 mM and 1.05 mM in rat and human EHTs, respectively [12]. This compares with 2.1 mM [13] and 3.0 mM [14] in adult rat and human muscle strips, respectively. (iv) The positive inotropic response to the beta-adrenergic agonist isoprenaline is less pronounced in EHTs than in adult hearts [9]. (v) Cardiomyocytes in native heart tissue are rod-shaped and couple end-to-end in intercalated disks which are very rich in gap junctions. This degree of spatial organization is not reached in EHT in which cardiomyocytes rather couple side to side [3] and, even under optimized conditions, display an abnormal length to width ratio (>11 compared to 7) [15].

Thus, a major goal in the field is to advance maturation of cultured cardiomyocytes in general and within EHT in particular. The simplest idea is waiting, and indeed culture times of several months are feasible for both rodent and human EHTs and led to improved maturation [9,15]. This is very likely facilitated by the beneficial 3D growth environment which enables interaction with fibroblasts and extracellular matrix [16], and optimal biomechanical loading [6,11]. However, most cardiac diseases occur in early or even late adult life, i.e. in cells decades older than their hPSC-derived counterparts in vitro, and long culture times are expensive and prone to infections, making this approach practically unfeasible. Growth factors and hormones, e.g. triiodothyronine (T3) [17], neuregulin-1β [18] or insulin-like growth factor-1 [19], and high ambient oxygen concentrations [20,21] promote cardiac maturation and 3D tissue development. Another method for tissue maturation is electrical field stimulation, which may play a natural role in tissues with electrical field strengths in the range of 0.01–2.0 V/cm [22]. Beneficial effects of pacing have been shown in cardiomyocyte-seeded collagen sponges [5] and EHTs [23], but the final tissue quality did not exceed that of standard fibrin EHTs cultured under high oxygen and in the presence of insulin and horse serum (with endogenous T3) [3].

In this study we established a protocol to electrically stimulate rat and human (induced pluripotent stem cell derived)-EHTs for several weeks. Stimulated rat EHTs were considerably stronger than controls, showed reduced spontaneous beating activity, a lower Ca^{2+}-sensitivity, a stronger inotropic response to isoprenaline and remarkably improved structure and ultrastructure. Likewise, force of human EHTs increased and their structural organization ameliorated considerably.

2. Material and methods

2.1. Generation of rat and human EHT

Rat engineered heart tissue (rEHT) was produced according to previously published protocols in a 24-well cell culture format [3,11]. All procedures were approved by the Hamburg Ethics Commission. In brief, ventricles from neonatal Wistar and Lewis rats (postnatal day 0 to 3) were digested repeatedly by DNAse and Trypsin. For one tissue strip of 100 μL 500,000 ventricular heart cells, fibrinogen, thrombin and DMEM were mixed and immediately cast into agarose casting molds around silicone posts protruding from a silicone rack. Within a period of two hours the fibrin polymerized and built an extracellular matrix for the ventricular heart cells. Afterwards the silicone racks each carrying 4 EHTs were transferred to a cell culture dish filled with rEHT medium. This consisted of DMEM (Biochrom F0415), 10% horse serum inactivated (Gibco 26050), 2% chick embryo extract, 1% penicillin/streptomycin (Gibco 15140), insulin (10 μg/mL, Sigma-Aldrich 857653), and aprotinin (33 μg/mL, Sigma-Aldrich A1153) and was changed three times per week.

Human engineered heart tissue (hEHT) was produced from human induced pluripotent stem cell (hiPSC) clone C25 which was a generous gift from the group of Laugwitz [24]. HiPSCs were differentiated into cardiomyocytes according to our previously published protocol for human embryonic stem cells (hESCs) [4]. Further enrichment was performed as recently described [25]. After the differentiation process 500,000 cells (cardiomyocyte content: 80–90%) were used for the generation of human EHTs (initial volume 100 μL). The procedure was carried out analogous to the production of rat EHTs with the exception that the fibrin matrix was supplemented with 10% Matrigel (BD Bioscience 356235) in the reconstitution mix and that EHTs from this lactate-enriched cell population were maintained in lactate-based EHT medium. This human EHT medium was changed daily and consisted of DMEM without glucose (Gibco 11966-025), 10% fetal calf serum inactivated (Biochrom S0615), 1% penicillin/streptomycin (Gibco 15140), insulin (10 μg/mL, Sigma-Aldrich 857653), aprotinin (33 μg/mL, Sigma-Aldrich A1153), and sodium L-lactate (4 mM, Sigma-Aldrich 71718). Both rat and human EHTs were maintained in 37 °C, 7% CO_2, and 40% O_2 humidified cell culture incubators throughout experiments and video-optical recordings. Aprotinin in the culture medium was required to prevent rapid dissolution of the fibrin matrix in the presence of serum.

2.2. Continuous electrical stimulation of EHT

EHTs were paced by mounting the silicone racks onto custom-made electrical pacing units. During development of these units their scaffold material was changed from acrylic glass over brass to stainless steel and electrode material from stainless steel to carbon. In the final version (Fig. 1A), which was exclusively used in this study, two stainless steel square bars (austenitic grade EN 1.4301, UNS S30400; Koch + Krupitzer, Germany) served both as conducting material and as scaffold for four pairs of carbon electrodes (CG 1290 Carbon Graphite Consulting Klein, Siegen, Germany). They were isolated from each other by polyamide plastic screws (GHW, Niederkrüchten, Germany). Only stainless steel connecting screws and nuts, rust-proof tools and unleaded tin-solder were used in the assembly process of the pacing units. A readily assembled pacing unit was narrow enough to fit into the wells of a standard 24-well dish (Fig. 1B). By connecting 6 pacing units in parallel 24 EHTs could be stimulated simultaneously. Yet, a significant disadvantage of electrical stimulation in buffer solutions is the formation of hypochlorous acid (HOCL), a strong oxidizer [26], and oxygen-derived free radicals [27]. Not to interfere with redox-reactions in cardiomyocytes we have refrained from supplementing our medium with an antioxidant such as sodium ascorbate [28], but employed known strategies to reduce the production of toxic metabolites and to optimize the stimulation setting. We used comparatively large carbon [29] electrodes in relation to the size of a single well which stood in a distance of 1 cm parallel to one another yielding a homogeneous electrical field. Symmetric biphasic pulses [23] of short duration [29] (4 ms overall, 2 ms in both polarities) were applied and both culture medium and pacing units were changed frequently (three times a week for rEHT and daily for human EHT). They were reconditioned by washing them at least 4 times 12 h in distilled water before autoclaving.

At day 4 of culture continuous electrical stimulation was initiated. The signals were generated by a Grass S88X Dual Output Square Stimulator (Natus Neurology Incorporated, Warwick, USA). An output voltage of 2 V (yielding an electrical field strength of 2 V/cm) in biphasic pulses of 4 ms was applied both to rEHT and hEHT.

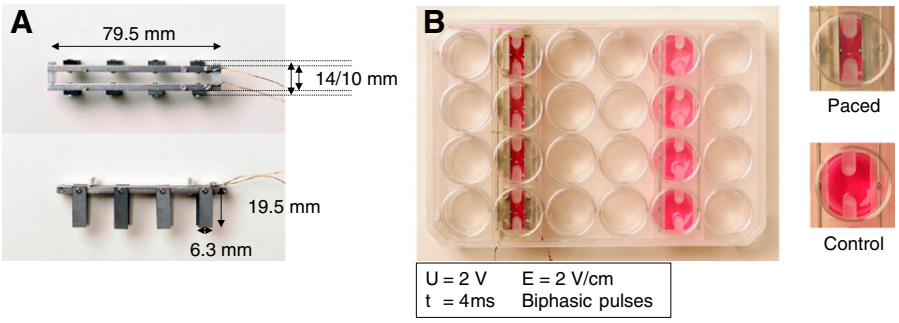

Fig. 1. Setup for electrical stimulation of EHTs. A) Pacing unit for 4 EHTs with carbon electrodes mounted on 1.4301 (V2A) stainless steel racks. View from above or the side. B) 4 paced EHTs (left side) and 4 control EHTs (right side) in a 24-well cell culture dish.

2.3. Contractility analyses by video-optical recordings

The geometry of pacing units was designed to enable recording of individual EHTs by a camera from the top. Recordings were obtained in an incubator with a glass roof. For this procedure the cell culture dishes remained closed facilitating a sterile method to repetitively record EHTs. Force and frequency were analyzed by customized software (CTMV, Pforzheim, Germany) from these videos. Details of the contractility analysis were published previously [3].

2.4. Light microscopy and immunohistochemistry

EHTs were fixed with formaldehyde both for conventional hematoxylin and eosin (H&E) staining and immunohistochemistry. After embedding in paraffin 4 μm sections were cut strictly longitudinally. H&E staining was performed according to standard protocols in an automated manner. For immunohistochemistry, staining conditions for each antibody were optimized on paraffin sections of adult rat hearts. 30 different combinations of antigen retrieval and antibody dilution were tested on the Ventana BenchMark XT (Roche) slide preparation system. Optimized conditions were: mouse anti-MLC2v monoclonal antibody (Synaptic Systems, 310111), dilution 1:2000, antigen retrieval: 30 min in citrate-buffer, pH 6.0; mouse anti-connexin-43 monoclonal antibody (BD Transduction Laboratories, 610061), dilution 1:200, antigen retrieval: 30 min in citrate-buffer, pH 6.0. All antibodies were visualized with the multimer-technology based UltraView Universal DAB Detection Kit (Roche). All microscopic images were taken on an Axioskop 2 microscope (Zeiss). Successive quantitative analyses were all carried out with ImageJ (http://rsbweb.nih.gov/ij) on MLC2v stained sections.

2.5. Three dimensional microscopy (confocal and 2-photon)

For confocal laser scanning and 2-photon microscopy, EHTs were processed as whole mounts. Each step, formaldehyde-fixation, blocking and permeabilization, incubation with primary antibodies and incubation with secondary antibodies, were performed for 24 h at 4 °C. Antibodies were used as follows: anti-dystrophin 1:250 (Abcam ab15277), anti-connexin-43 1:250 (BD Transduction Laboratories 610061), Alexa Fluor 488 goat anti-mouse 1:800 (Invitrogen A11001), Alexa Fluor 546 goat anti-rabbit 1:800. Nuclei were counterstained with DAPI 1:1000 (Sigma-Aldrich D9542). The blocking solution contained TBS 0.05 M, pH 7.4, 10% FCS, 1% BSA, 0.5% Triton X-100; the antibody solution contained TBS 0.05 M, pH 7.4, 1% BSA, 0.5% Triton X-100. Confocal microscopy was performed on a Zeiss LSM 510 META System, 2-photon microscopy on a LaVision Biotec TriM Scope equipped with a tunable femtosecond-pulsed titanium-sapphire-laser (wavelength range 700–920 nm, 80 MHz, MaiTai, Spectra Physics, Germany). For the latter EHTs were excited at a wavelength of 770 nm and emission photons were split by a 610 nm dichroic mirror before being detected by two photomultiplier tubes. DAPI fluorescence and Alexa Fluor 488 fluorescence of connexin-43 were collected through a 510/55 nm interference filter before being detected by a blue sensitive PMT (Hamamatsu H 6780-01). Alexa Fluor 546 fluorescence photons of dystrophin passed a 655/40 nm interference filter and were detected by a red sensitive PMT (Hamamatsu H 6780-20). 150 μm × 150 μm square at the surface and right in the middle of an EHT was chosen as first plane ($z = 0$ μm). Then images of planes below were acquired in 2 μm steps until the working distance of the objective (Zeiss EC Plan-Neofluar, 40×/1.3 oil DIC, Carl Zeiss, Germany) was reached ($z \approx 210$ μm). The number of connexin-43 positive structures and the sum of connexin-43 intensity were analyzed in a cube $x = y = z = 150$ μm with appropriate filters in Imaris 7.6.1 by a blinded investigator. Likewise, the thickness of the compact cardiomyocyte layer of EHTs was measured by a blinded investigator.

2.6. Electron microscopy and dependent analyses

Prior to fixation EHTs were incubated with 2,3-butanedione monoxime (BDM, Sigma-Aldrich B0753) at 30 mM in PBS for 10 min to stop EHT contraction and to allow for sarcomere relaxation. EHTs were fixed overnight in 0.36% glutardialdehyde and postfixed with 1% osmium tetroxide for 2 h. Samples were dehydrated and embedded in epon. 90 nm sections were mounted onto electron microscopy grids and stained first with 4% aqueous uranyl acetate in a 1:1 solution with ethanol for 30 min, washed in demineralized water, stained for 30 min with lead citrate, re-washed in demineralized water and allowed to dry. Analysis of samples was performed using a Jeol 1200 transmission electron microscope, operated at 100 kV. Images were recorded using a Tietz Fastscan CCD camera with resolution of 1024 × 1024 pixels.

Z-band width was measured with ImageJ in 50 representative Z bands at 7500× magnification according to a previously published method [30]. Stereological analyses were also performed using ImageJ. Five representative electron micrographs (one heart or EHT per condition) at 1000× magnification were chosen for analysis per sample; the nucleus was excluded from all samples.

2.7. Concentration-response curves

The force of rEHTs as a function of external Ca^{2+}-concentration and their response to isoprenaline were analyzed in a modified video-optical recording and analysis system [12]. The stimulator used as well as the electrical field strength and pacing mode were the same as in Section 2.2; the frequency was set to 2 Hz. In contrast to the system described in Section 2.3, all wells were continuously perfused (37 °C, 95% O_2, 5% CO_2) with Tyrode's solution (in mM: NaCl 120, KCl 5.4, $MgCl_2$ 1.0, $CaCl_2$ 0.05–1.8, NaH_2PO_4 0.4, $NaHCO_3$ 22.6, glucose 5.0, Na_2EDTA 0.05, ascorbic acid 0.6; 6 ml/min). The external Ca^{2+}-concentration was increased stepwise (0.05–0.1–0.2–0.4–0.6–1.0–1.8 mM) every 20 min; the force was measured directly before the next step. The additional force by the administration of isoprenaline (100 nM) was determined at 0.1 mM external Ca^{2+}.

2.8. Whole transcriptome analysis

RNA from five control and five paced rEHT was isolated as previously described [11], transcribed, amplified and hybridized on the Rat Gene 1.0 ST Array (Affymetrix) according to the manufacturer's protocols. Arrays have been quantile-normalized with respect to the probe GC content using the RMA algorithm. Not or low expressed transcripts have been removed by a maximum expression cutoff <100. The data filtering led to sets of 14,505 of 29,214 meta-probe sets. After normalization the arrays have been checked for outliers using the principal component analysis (PCA), a correlation dispersion matrix and normalized Eigenvector scaling. No outlier was found in the first four principle components (PCs) representing 67.3% of the dataset variance. The first PC is mainly driven by paced to control differences (Fig. 6C, X-axis). The analysis of differential expression of summarized gene level expression has been performed using the t-test approach of the Partek Genomic Suite version 6.6 followed by a FDR multiple testing correction; only FDR corrected p-values are reported below. The pathway analysis was conducted with IPA (Interactive pathway analysis of complex omics data, Release 2013-05, Ingenuity Systems). Differentially expressed in IPA was defined as >1.5 fold upregulation or <0.66 fold downregulation and an FDR-corrected p-value <0.05.

2.9. Statistics

Results are presented as mean ± SEM unless otherwise stated (Fig. 5P). All statistical tests were performed in GraphPad Prism version 5.02. 1-way ANOVA and Dunnett's multiple comparison post test (to compare to controls) or 1-way ANOVA and Tukeys's multiple comparison post test (to compare all groups) were used for more than 2 groups, or Student's unpaired t test for 2 groups. The ends of whiskers in the boxplots represent the minimum and maximum of all of the data. 2 × 2 contingency tables were analyzed with Fisher's exact test. $p < 0.05$ or less was considered statistically significant. p-Values are displayed graphically as follows: * $p < 0.05$, ** $p < 0.01$, *** $p < 0.001$, ns = not significant.

3. Results

3.1. Establishment of the experimental model

The pacing units (Fig. 1A) were constructed in a way that EHT contractile activity could be video-optically recorded with electrodes inserted into the 24-well dish (Fig. 1B). The blue squares in the still image (Fig. 2A) indicate the positions to analyze the deflection of the silicone posts when EHTs were contracting. Contractile force was calculated from the deflection of the posts (Supplemental Fig. S1) and plotted over time (Figs. 2B–C). Non-stimulated rEHT (Fig. 2B) typically contracted in bursts of 10–30 s length and a frequency of ~4 Hz, followed by resting periods of 10–30 s. The electrical pulses of the stimulator (blue lines in Fig. 2C) induced contractions, which were easily discernible in the resting periods, but also regularly observed in the bursts. The electrical field strength excitation threshold varied little between individual EHTs (1.6–1.8 V/cm). At 2 V/cm field strength all EHTs were definitively paced. Therefore this setting was kept in biphasic pulses of 4 ms duration throughout the experiments. The current was 60–65 mA per pacing unit (with 4 EHTs), thus 6 pacing units in parallel (24 EHTs) required a current of 360–390 mA. Of note, the scaffold material of the pacing units was of critical importance. Early experiments with brass led to considerable heavy metal concentrations in the culture medium, although the scaffold was not in direct contact with the medium or the EHTs, and limited the lifetime of permanently paced EHTs to less than a week. Stainless steel (austenitic grade EN 1.4301, UNS S30400) turned out to be an optimal material with its excellent corrosion resistance, biological compatibility and a sufficient electrical conductivity σ of 1.4 S/m. The spontaneous beating frequency of rEHT during the bursts (~4 Hz) could be overridden by setting the stimulator at 5 Hz, but this led to a decline in contractile force within hours (Fig. 2D).

3.2. Impact of chronic pacing on contractile parameters of rat EHT

Due to the adverse effects of pacing rEHTs at 5 Hz, the effect of constant pacing with a low frequency was tested. In the natural time course

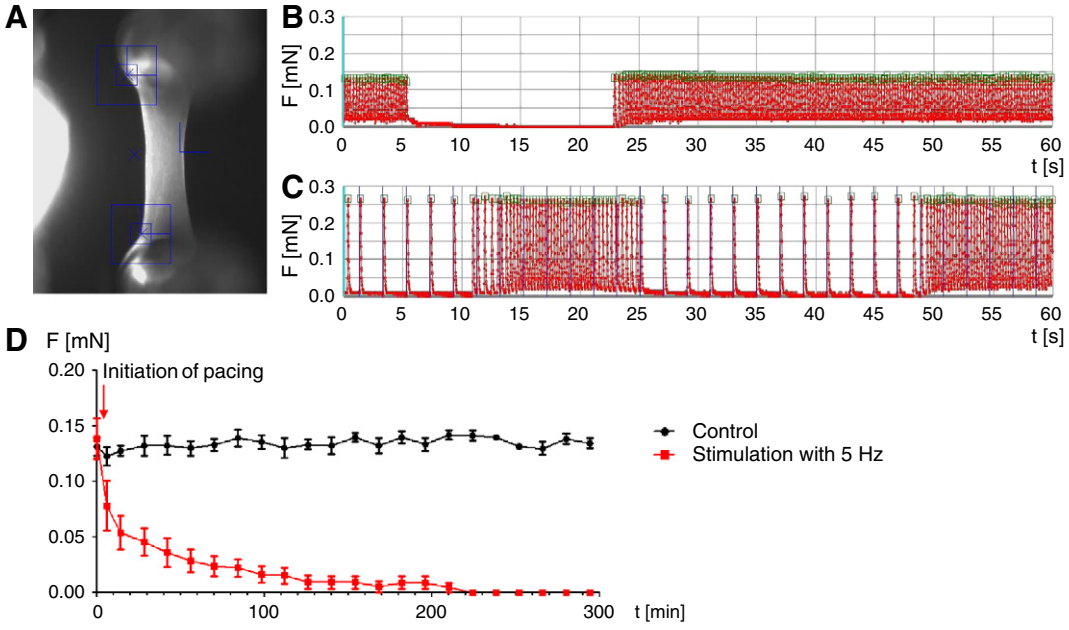

Fig. 2. Force measurements of stimulated rat EHTs. A) Still image of an EHT. Blue squares indicate positions which are used to analyze EHT contractions. B) Control rEHTs beat in bursts with a rate of approximately 4 Hz and 10–30 s duration alternating with resting periods of 10–30 s duration. C) Stimulation of rEHTs with low frequency (0.5 Hz, blue lines). D) Force of EHTs over time. Stimulation with 5 Hz led to a rapid contractile deterioration.

of rEHTs there is no beating at day 0, start of uncoordinated beating around day 4 and coherent beating of the entire tissue construct around day 8. At day 4 we initiated constant pacing at 0.5 Hz which could be attained throughout the lifetime of a rEHT without evidence of toxicity even during a maximum pacing duration of 32 days. Continuously paced (cp) rEHTs developed increasingly higher forces than control EHTs. The curves started to deviate from each other at 7 days of pacing (11 days of culture). After 18 days of pacing cp-rEHTs generated 85–90% higher forces than control rEHTs. The higher contractile forces were observed independent of whether rEHTs in the pacing group were actively paced (cp-p) or beat spontaneously during the measurements (pacer off, cp-s; Figs. 3A–B). Throughout pacing diameters of paced rEHTs decreased to greater extents than that of non-paced rEHTs. Accordingly, force normalized to cross-sectional area of rEHTs almost tripled (Fig. 3C). Although series of rEHT were slightly different in terms of absolute force, the force-increasing effect of chronic pacing was seen in all ($n = 5$) independent experimental series. For the sake of clarity only one representative series of rEHT is displayed in Figs. 3A–D, all other series can be found in Supplemental Fig. S2 as well as fractional shortening in Fig. S3A. All series taken together cp-rEHT developed 2.2× higher forces (0.26 mN, $n = 50$) than control rEHT (0.12 mN, $n = 46$) as measured on days 20–22.

After the onset of coherent beating around day 8 of culture, rEHTs usually had the highest spontaneous beating frequencies. The frequencies dropped both in control and paced EHTs. In some experimental series all paced EHTs completely lost their spontaneous beating activity (Fig. 3D) although they were still fully electrically stimulable. Overall, the loss of spontaneous beating activity was more frequent in paced than in non-paced rEHT (Fig. 3E). Furthermore, the frequency of beating during bursts was lower in the pacing groups (control: 3.89 Hz; cp-s: 3.28 Hz; cp-p: 3.35 Hz; Fig. 3F) measured at day 15. At later time points the burst pattern usually disappeared.

3.3. Structural and ultrastructural changes of paced rat EHT

To evaluate whether the functional improvement of paced rEHT had a structural correspondent, rEHTs were analyzed by several microscopic techniques. As rEHT usually reveals a low cardiomyocyte density in the center, meridional sections of paraffin embedded rEHTs were analyzed with conventional light microscopy (Fig. 4A). Three week paced rEHTs were thinner than their non-stimulated counterparts (as reported above, Fig. 3C). Additionally, they were more densely packed with cells. Regular cross striation indicated that cardiomyocytes were more mature in paced rEHTs than in controls (Figs. 4B–C). An antibody against myosin regulatory light chain 2, ventricular isoform (MLC2v) exclusively stained the ventricles (positive control) in neonatal (Fig. 4D) and adult rat heart (Fig. 4E), confirming its high specificity for MLC2v. Staining of rEHTs revealed that chronic pacing increased the length, width and density of cross striated MLC2v-positive cardiomyocytes (Figs. 4F–G, Supplemental Figs. S4A–E). Remarkably, the cell density gradient between the edges and center commonly observed in control rEHTs (Figs. 4B, F, I) was largely reduced in paced rEHTs (Figs. 4C, G, J).

The morphological and functional data presented so far suggested a higher degree of maturation in paced rEHTs and prompted us to stain for the gap junction protein connexin-43, which showed the typical intercalated disk signal in adult rat heart sections (positive control, Fig. 4H). Whereas connexin-43 staining was considerably stronger in paced than in control rEHTs, especially in the central regions, it did not show a typical intercalated disk pattern in rEHTs in either group (Figs. 4I–J). Instead, it was detectable in small punctae throughout the cardiomyocyte cell membrane. This finding was confirmed in confocal images of near-surface regions of control (Fig. 5A) and paced rEHTs (Fig. 5B), which showed gap junctions at lateral contact points of two cardiomyocytes. As the penetration depth of conventional confocal laser scanning microscopes for rEHT was limited to ~50 μm, we next investigated them with two-photon microscopy. The first imaging plane was chosen at the surface ($z = 0$ μm) directly in the middle of an rEHT (Fig. 5C). There were more connexin-43^{+}-dots (+117%, Fig. 5D) and a greater overall connexin-43 intensity sum (+343%, Fig. 5E) in a cube analyzed with an edge length of 150 μm. Furthermore, by obtaining images up to the technical limit of $z \sim 210$ μm the thickness of compact cardiomyocyte layer was determined in control (85 μm) and paced rEHT (132 μm, +56%; Fig. 5F). All two-photon microscopy dependent analyses were carried out by an experienced user which was blinded toward the groups.

Electron microscopic analyses by an investigator blinded to the identity of the samples extended the evidence for better cardiomyocyte maturation in paced rEHTs. Adult rat myocardium served as positive

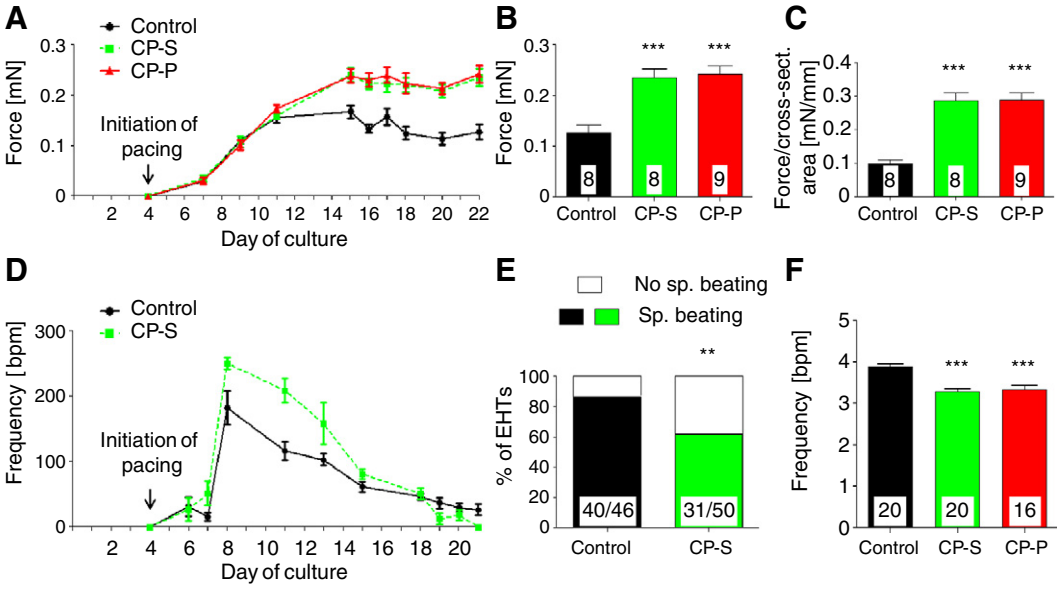

Fig. 3. Impact of chronic pacing with 0.5 Hz on contractile parameters of rEHT. A) Force development of rEHT over time, B) contractile force at day 22 and C) contractile force normalized to cross sectional area of rEHTs at day 22. D) Typical frequency development of rEHTs under chronic stimulation. E) Percentage of EHTs (from 5 independent experiments) which beat spontaneously (or not) at the last day of the pacing experiments (day 21–36). F) Frequency of beating during bursts at day 15. CP-S stands for chronic pacing group in which the stimulator was switched off transiently for measurement (i.e. spontaneous beating, depicted in green). CP-P are the same EHTs but with stimulator switched on (i.e. paced, depicted in red).

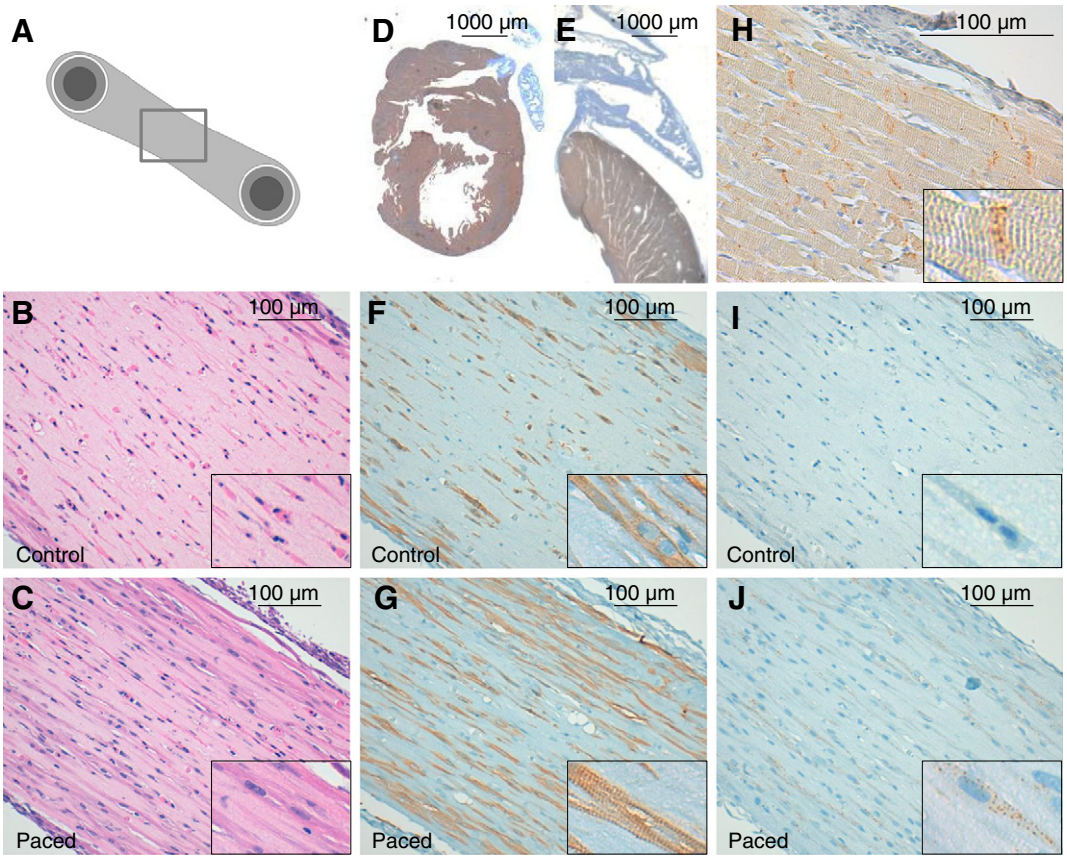

Fig. 4. Microscopic images of control and paced rEHTs. A) Pictograph of an rEHT with the location of the microscopic sections depicted (B, C, F, G, I, J). B) Control and C) paced rEHT in H&E staining. D) Neonatal rat heart and E) adult rat heart in an immunohistochemical staining for MLC2v. F) Control and G) paced rEHT immunohistochemically stained for MLC2v. H) Immunohistochemistry for connexin-43 staining on adult rat heart, I) control and J) paced rEHTs. All insets show 2× larger magnification.

control for overall sarcomere organization (Fig. 5G), mitochondria (Fig. 5H) and sarcomeric details (Fig. 5I). The ultrastructure of cardiomyocytes in control rEHTs varied widely, ranging from hardly discernible sarcomeres in the center of the EHT to relatively well developed ones in cells from the edge while myofibrils appeared untensioned and often adapted to the shape of mitochondria (Fig. 5J). Mitochondria without any cristae and small membrane-bound vesicles, presumably derived from the inner mitochondrial membrane, were found in the center of control EHTs (Fig. 5K), but not at the edges. The discrepancy between center and surface was also observed regarding Z-band definition and A–I transition (Fig. 5L). Myofibrils in paced EHTs were regularly found in a straight line and aligned with mitochondria, albeit the high degree of organization seen in native tissue was not achieved. The ultrastructure was remarkably better than in control rEHT with clear M-bands (Fig. 5M) and no mitochondria with the vesicle-like phenotype, but with regular cristae (Fig. 5N). Still, overall mitochondria in rEHT appeared often larger and less organized than in native heart, regardless of pacing. A–I transition was more defined in paced rEHT (Fig. 5O) than in control rEHT (and even native tissue). Moreover, Z-bands were sharper in paced rEHTs than in controls. This was reflected by a smaller standard deviation of the Z-band widths. Besides this, there was a tendency toward a smaller mean Z-band width in paced rEHTs (Fig. 5P). Finally, cell composition was assessed by stereological analysis. The nucleus was excluded from this analysis as its volume can vary dramatically depending on where the cell is sectioned when the sample is prepared. Rat adult cardiomyocytes comprised around 50% sarcomeres, which is higher than in rEHT. Paced rEHT had a tendency toward a higher sarcomere fraction compared to control rEHT (34% vs. 24%, ns). While the fraction of mitochondria in rEHTs was similar to native tissue, their cytoplasm fraction was considerably higher (Fig. 5Q).

3.4. Ca^{2+}-concentration and isoprenaline response of paced rat EHT

An important aspect of heart tissue maturation is the force response to external Ca^{2+}-concentration and the prototypic inotropic receptor agonist isoprenaline, i.e. the dynamic range. The force developed by rEHTs increased with rising Ca^{2+}-concentrations in both groups, and again paced rEHTs generated double the force of control rEHTs (see Fig. 3B). Compared to control rEHTs, the Ca^{2+}-response curve was shifted to the right in paced rEHTs by 0.055 mM or 40% (Fig. 6A). Isoprenaline at a maximally effective concentration of 100 nM evoked a stronger increase of force in paced rEHTs than in control rEHTs, both in absolute (0.17 mN vs. 0.11 mN) and relative terms (+165% vs. +100% of baseline; Fig. 6B).

3.5. Gene expression analysis

A whole-genome gene expression analysis of control and paced rEHTs was performed to test whether the functional and structural improvements of paced rEHTs were accompanied by transcriptional alterations. 14,505 transcripts (of a total of 29,214 annotated transcripts) were sufficiently highly expressed in rEHT to be detected. A principal component analysis of the global expression revealed that the first principle component represented 35% of the dataset variance. This was mainly driven by control to paced differences. The full separation of the two groups indicated strong effects of pacing on global gene expression (Fig. 6C). As force of paced rEHTs was augmented and frequency and bursts reduced, all 59 plasma membrane ion channel components in the expression analysis were scrutinized. By far the strongest upregulated channel subunit was KCNJ8 coding for the $K_{ir}6.1$ protein (FC 2.61; $p = 0.004$). Being part of the heterooctameric complexes of inwardly-

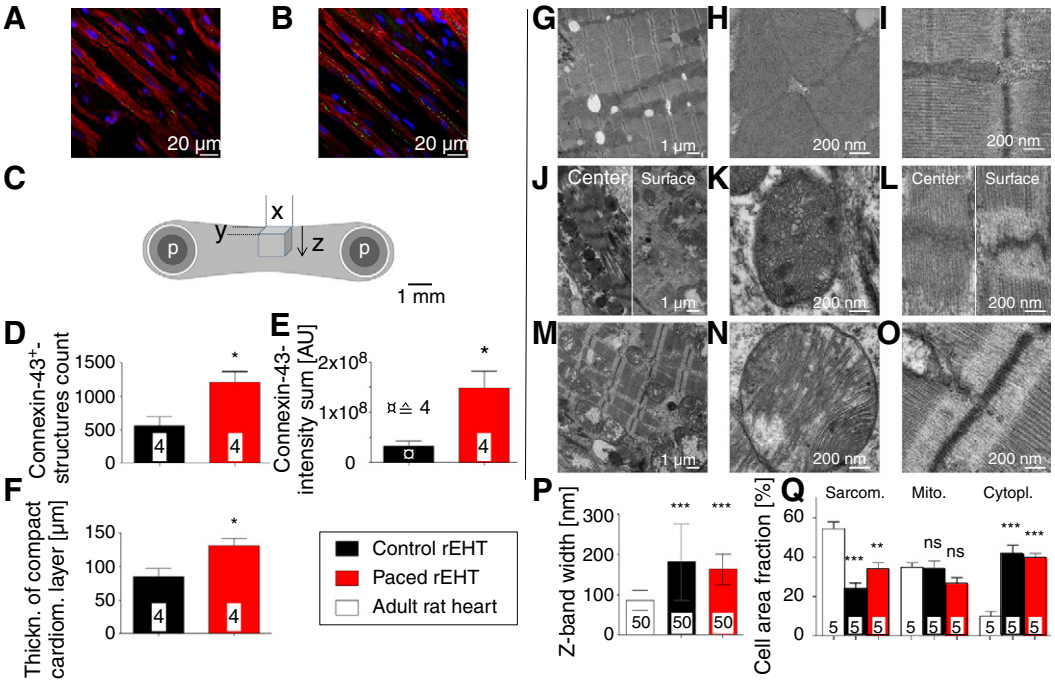

Fig. 5. Three-dimensional and electron microscopy. A) Merged confocal analysis of an area close to the surface of a control and B) a paced rEHT stained with an antibody against dystrophin (red), connexin-43 (green) and with DAPI (blue). C) Pictograph of an rEHT displaying the cuboid which was analyzed by two-photon excitation microscopy. x and y were 150 µm, the first plane (z = 0) was at the surface of an EHT right in the middle between the two silicone posts (p). Maximum depth (i.e. in z-direction) was 210 µm. D) Number of connexin-43 positive dots and E) sum of connexin-43 intensity, analyzed by two-photon microscopy in a cube (x = y = z = 150 µm). F) Thickness of compact cardiomyocyte layer, also measured with two-photon microscopy. Electron microscopy of adult rat heart (G–I), control rEHT (J–L) and paced rEHT (M–O). Overview of the cardiomyocyte ultrastructure (G + J + M). Mitochondria (H + K + N). A–I-transition and Z-band (I + L + O). P) Quantification of Z-band width (mean ± SD, n = 50). Q) Stereological analysis of the composition of cardiomyocytes (n = 5).

rectifying ATP-sensitive potassium channels it can stabilize resting membrane potential, thus reducing ectopic activity and spontaneous beating frequency. Another determinant of pacemaking activity is the I_f-current. The main isoform of the respective channel forming subunits in pacemaker tissues, HCN4, was strongly downregulated (FC 0.48; p = 0.001). Endothelin-1, a strong inducer of fibrosis, was the second most strongly downregulated of all genes (FC 0.20; p < 0.001). Ctgf (connective tissue growth factor), a downstream fibrotic mediator, was also downregulated (FC 0.45; p = 0.001). Conversely, proteins involved in the breakdown or remodeling of extracellular matrix were upregulated, e.g. MMP9 (FC 2.06; p = 0.014) or showed a trend toward upregulation (MMP3; FC 2.32; p = 0.077). The expression level of collagen-1 or fibroblast markers such as periostin remained unchanged. Upregulation of connexin-43 (= Gap junction protein, alpha 1, Gja1; FC 1.49; p = 0.022) confirmed the increase in connexin-43-positive structures in paced rEHTs. The SR-Ca^{2+}-ATPase Serca2a was unchanged, but its inhibitor phospholamban decreased by 18% (FC 0.82; p = 0.0037).

A pathway analysis (IPA, Ingenuity Systems) of the gene expression of paced and control rEHTs was conducted for an unbiased approach to its interpretation. It unambiguously revealed that chronic pacing initiated an inflammatory response in rEHT. The top network was "immune cell trafficking"; top associated disease and disorder "inflammatory response"; top cellular function "cellular movement"; top canonical pathway "granulocyte adhesion and diapedesis", $p < 10^{-12}$ followed by "agranulocyte adhesion and diapedesis", $p < 10^{-11}$ and top upstream regulator TNF-alpha, $p = 2.2 \times 10^{-31}$ (Supplemental Table S1).

3.6. Function and structure of human EHT by chronic pacing

The findings in rEHTs were applied to hiPSC-derived hEHTs with the same settings as for rEHTs. However, hEHTs differed in their spontaneous beating pattern, showing very regular beating ~1.5 Hz in the beginning and a drop to around 1 Hz during the first 14 days of culture (Fig. 7A). For this reason we tested two pacing protocols, pacing at 0.5 Hz for the entire period and pacing at 2 Hz during the first week and 1.5 Hz thereafter, thus ensuring permanent overstimulation of the spontaneous beating activity (Fig. 7B). Culture medium was changed daily assuming more hypochlorous acid to be produced by the higher pacing rate. Stimulated hEHTs developed higher forces than controls after 4–6 days of stimulation (Fig. 7C). Whereas differences did not reach statistical significance for the low frequency group, the high frequency paced hEHTs had markedly higher forces than unstimulated control hEHTs (0.083 mN vs. 0.056 mN, +48%, Fig. 7D), both under spontaneous beating (cp-s) and pacing (cp-p). Fractional shortening increased accordingly and reached 7% in paced hEHTs (Supplemental Fig. S3B).

The structure of hEHTs was examined after 10 days of pacing with high frequency. H&E stained paraffin sections revealed that hEHTs in general were less mature than their rEHT-counterparts, i.e. overall nuclear density was higher, nuclei were mainly round, the cytoplasm-to-nucleus ratio was lower as was orientation and demarcation of cardiomyocytes from surrounding matrix (Fig. 8A). However, paced hEHTs compared to unpaced controls exhibited a much better muscular network of longitudinally oriented cardiomyocytes with higher cytoplasm-to-nucleus ratio (Fig. 8B). Staining with the MLC2v antibody (Figs. 8C–D) confirmed that cardiomyocytes were longer both in absolute (Fig. 8E) and relative terms (expressed as ratio to cardiomyocyte width, Fig. 8F), were slightly slimmer i.e. less round, (Supplemental Fig. S5), were more stringently aligned in paced hEHTs (smaller scatter in Fig. 8G) and exhibited clearer cross-striation. Furthermore, paced hEHTs had more contractile mass relative to cell-free matrix than control hEHTs (Fig. 8H).

4. Discussion

In the presented study, we investigated the hypothesis that long-term electrical stimulation of rat and human (hiPSC-derived)-EHT

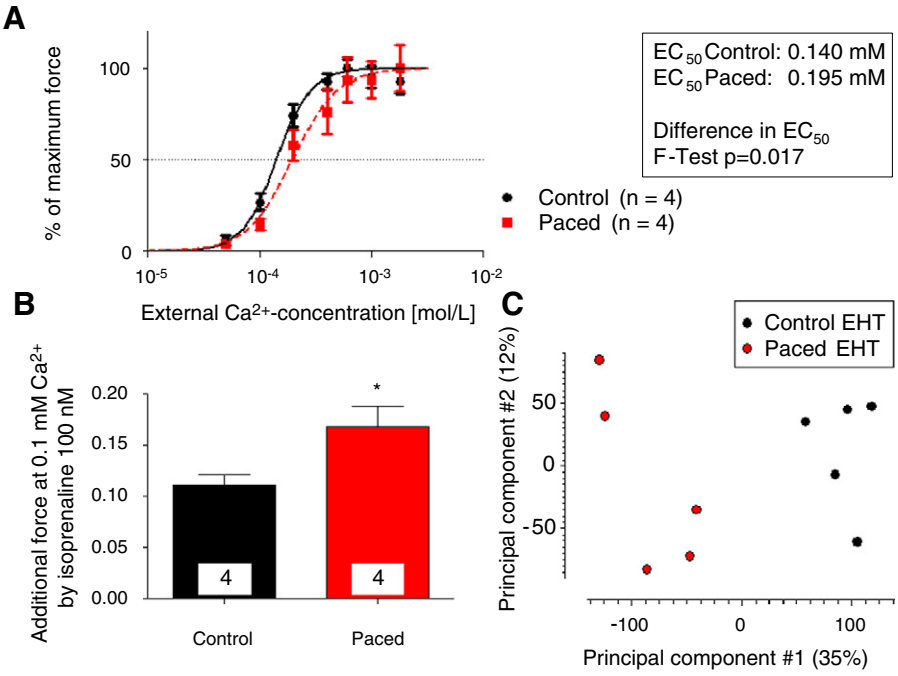

Fig. 6. Concentration-response curves and gene expression analysis of rEHTs A) Force of control rEHTs (black dots) and paced rEHTs (red squares) depending on external Ca^{2+}-concentration. Forces were normalized to maximum control EHT force or maximum paced EHT force, the latter being twofold higher in absolute values. B) Additional force of control and paced EHTs by stimulation with 100 nM isoprenaline at 0.1 mM external calcium concentration. The baseline force at 0.1 mM Ca^{2+} was 0.055 mN for control and 0.064 mN for paced rEHTs. C) Principal component analysis of gene expression analysis of 5 control and 5 paced rEHTs. Principal component #1 is driven by control to paced differences explaining 35% of the dataset variance.

improves contractile properties and induces maturation. Our findings support this hypothesis.

Field stimulation of isolated adult ventricular cardiomyocytes can preserve their mature phenotype for up to 72 h [31]. This principle has been adopted to engineered myocardial tissue by the groups of Vunjak-Novakovic and Radisic [5,32–34] and the group of Tong and Ralphe [35]. In our study, continuous pacing of rat (at 0.5 Hz) and human EHT (2 Hz/1.5 Hz) was continued for more than 4 weeks without obvious signs of toxicity. This is much longer than usually reported in the literature (5–9 days) [5,23,29]. Importantly, we designed the pacing units and the protocol under the premise that neither medium conditions nor our video-optical recording system [3,4] had to be changed which enabled us to monitor functional parameters of EHT throughout the entire culture time under sterile conditions. The scaffold material is of great importance for long-term pacing as heavy metal poisoning led to complete beating inactivity when using less precious material than 1.4301/S30400 stainless steel. In contrast to many other published techniques upscaling is easy, but demands high power stimulators. We regularly paced 24 EHTs in parallel which demanded a current of 380 mA. Our protocol can be easily adopted in any laboratory working with cardiac tissue constructs.

A notable advantage of the new system compared to earlier ones [29,32] is that it allows repeated measurements of contractile function under continued pacing. Contractile forces and fractional shortening of the hydrogel-based EHT are already high under nonstimulated conditions ($FS_{rat\ EHT}$ ~ 10%, $FS_{human\ EHT}$ ~ 5%), but rat EHTs took off after one week of pacing and reached their maximum after around three weeks of pacing with double the force of nonstimulated EHT. Human stimulated EHTs (at 2 Hz/1.5 Hz) surpassed their controls after 4–5 days and reached ~50% higher forces after 10 days of continuous pacing. Of note, our stimulation frequencies were in the physiological range and thus much lower than frequencies reported by others (up to 6 Hz in human cardiac tissue constructs [32]).

The mechanisms underlying the improved function of chronically paced EHTs likely involve both quantitative and qualitative alterations — recruitment of more cardiomyocytes participating in the coordinated contraction of EHTs and improved function of single cardiomyocytes. Arguments for the former are much denser and evenly distributed cardiomyocyte network throughout the diameter of paced EHTs (Figs. 4 and 8), higher connexin-43 density and intensity (Figs. 4 and 5), indicating better coupling [36], and a thicker compact cardiomyocyte network as revealed by two-photon-microscopy (Fig. 5). Presumably, electrical field stimulation either directly or via improved coupling leads to better recruitment of cardiomyocytes in the center of EHTs, which then contributes to higher force generated. Of note, the more even distribution of thick muscle strands throughout paced EHTs provides strong argument against the assumption that hypoxia or nutrient deprivation accounts for uneven muscle tissue distribution in control EHTs. Another interesting aspect is that connexin-43, though clearly more prevalent in cardiomyocytes of paced EHTs, did not acquire the classical concentration in intercalated discs at end-to-end cell connections. The reason may be the simultaneous and diffuse excitation by field stimulation compared to the directed stimulation in native hearts.

In addition to better cardiomyocyte recruitment, several data argue for qualitative changes in cardiac myocyte or cardiac tissue function in paced EHTs. (i) The shift of the Ca^{2+}-concentration response curve to more physiological concentrations and the stronger isoprenaline response indicates improved maturation. (ii) Gene expression of Serca2a, a critical regulator of intracellular Ca^{2+}-cycling [37], did not change, but its endogenous inhibitor phospholamban was downregulated, putatively leading to higher activity of Serca2a. (iii) Spontaneous beating activity (a sign of immaturity in ventricular myocytes [7]) ceased 3-times more often in paced than in control EHTs (Fig. 3). Variability between batches (2/5 stopped beating) suggests that slight variations in the age of the pubs used for the preparation of cells or contamination with pacemaking cells influence the beating activity. HCN4, the main ion channel isoform generating I_f-currents in pacemaking cardiac cells [38], was strongly downregulated in paced rEHTs, while KCNJ8 which gives rise to membrane potential-stabilizing I_{K1} currents, was upregulated. (iv) Continuously stimulated EHTs were longer and slimmer in the resting state (Supplemental Fig. S6). Given the defined elastic properties of the silicone

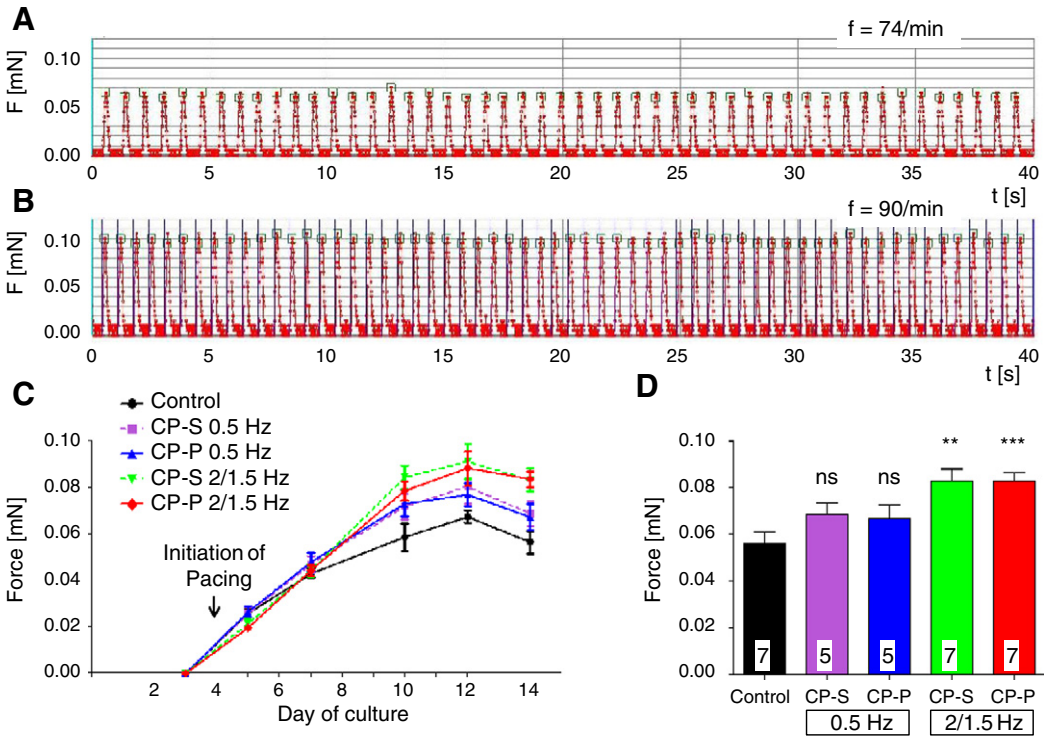

Fig. 7. Impact of chronic pacing with low and high frequency on contractile parameters of hEHTs. A) Control hEHTs reveal a very regular beating pattern. B) Stimulation of hEHT with high frequency (1.5 Hz, blue lines). C) Force development of hEHTs over time and D) after 10 days (day 14 of culture) of chronic pacing.

posts, longer resting length provides direct evidence for lower stiffness, either due to more complete relaxation (e.g. because of increased Serca2a function) and/or a decrease in extracellular matrix (ECM). Endothelin-1 increased EHT stiffness by inducing fibrosis [11]. Conversely, chronic pacing led to profound downregulation of endothelin-1 and its downstream effector Ctgf, suggesting less ECM in paced EHTs. (v) Finally, light and 2-photon microscopy revealed a higher cardiomyocyte density and more even distribution in stimulated rEHTs. Analysis by electron microscopy revealed that the sarcomere structure was very homogenous and all of its subregions (including M-band) were clearly discernible. Therefore, chronic stimulation appeared superior to shorter periods of pacing [5] or mechanical load alone [2]. The microscopic differences between

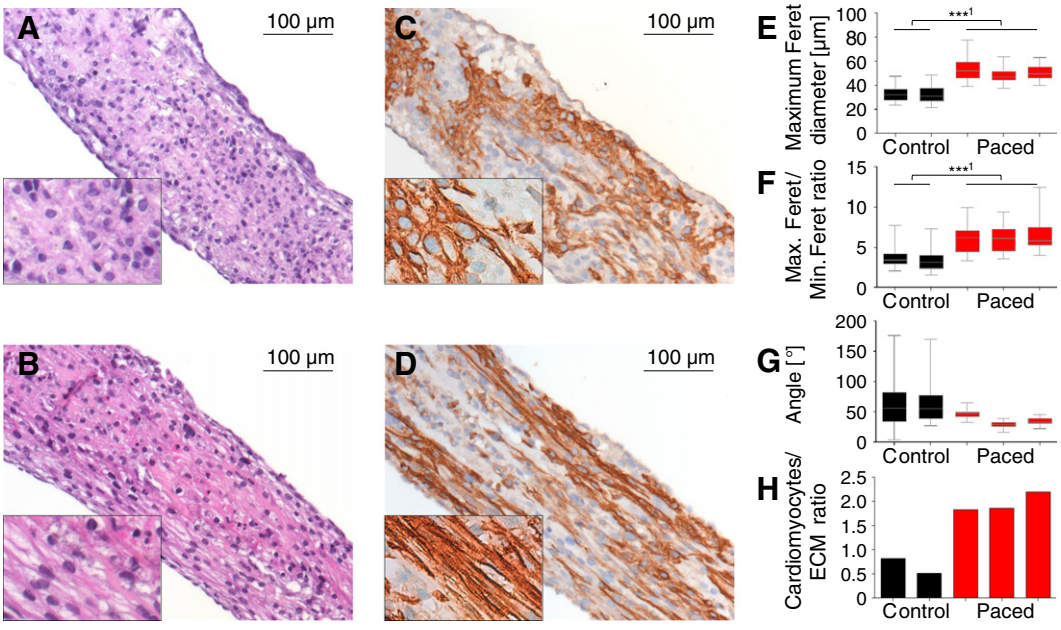

Fig. 8. Microscopic images and quantitative analyses of control and high frequency (2 Hz/1.5 Hz) paced hEHTs. A) Control and B) paced hEHT in H&E staining. C) Control and D) paced hEHT immunohistochemically stained for MLC2v. All insets show 2× larger magnification. E) Maximum Feret diameters and F) ratios of maximum to minimum Feret diameters and G) angle of maximum Feret diameter of cardiomyocytes to the horizontal line of two control and three paced hEHTs. 25 cardiomyocytes were analyzed per hEHT in E–G. H) Ratio of section area covered by cardiomyocytes to ECM area. [1]Each pair of hEHTs was tested with Tukey's multiple comparison post test. p-Values for all differences of control and paced hEHTs were < 0.001. There were no differences when testing a pair of control or a pair of paced hEHTs.

stimulated and non-stimulated hEHTs were even greater, likely related to the fact that the tissue structure of non-stimulated hEHTs was inferior to non-stimulated rodent EHTs. Under pacing, their structure improved remarkably. The cytoplasm: nucleus ratio increased, cardiomyocytes aligned along the long axis of an EHT and were longitudinal in shape, and cross striation improved.

Taken together, we observed that hydrogel-based EHTs benefit from long-term electrical stimulation and reach an unprecedented cardiac tissue structure and function, including considerably higher force, denser cardiomyocyte network with improved gap junction coupling, a more physiological response to external Ca^{2+}, increased inotropic response to isoprenaline and a well-developed sarcomeric ultrastructure. Yet, stimulated EHTs are still inferior to native adult cardiac tissue. Force normalized to cross sectional area is lower, the sensitivity to external Ca^{2+} is still too high and mitochondria are immature. Of note, the gene expression analysis revealed an inflammatory pattern, likely reflecting a protective reaction against pacing-induced oxidative stress [39]. This illustrates once again that electrical stimulation induces electrochemical stress and that the improved phenotype of chronically paced EHTs is likely the net outcome of beneficial and detrimental effects of pacing, opening the way for further improvement.

Funding sources

This study was supported by funds from the Deutsche Forschungsgemeinschaft (HA 3423/3-1, Es 88/12-1), Deutsche Herzstiftung (F/13/10), European Union (FP7 Projects Angioscaff 214402 and Biodesign 262948), Werner Otto Stiftung and the DZHK (German Centre for Cardiovascular Research, a part of the German Centres of Health Research, which is a BMBF (German Ministry of Education and Research) initiative. HEXT is supported by funds from the Freie und Hansestadt Hamburg.

Acknowledgments

We thank Jutta Starbatty, Thomas Schulze and June Uebeler for their excellent general technical assistance, Bülent Aksehirlioglu for helping in manufacturing the electrical pacing units, Dagmar Claussen for taking photographs, Kristin Hartmann, Melanie Neumann and Susanne Krasemann of the HEXT Mouse Pathology Facility, Aya Shibamiya and Sandra Laufer of the HEXT Stem Cell Facility, and Antonio Virgilio Failla of the HEXT UKE Microscopy Imaging Facility for assistance in 2-photon microscopy.

Appendix A. Supplementary data

Supplementary data to this article can be found online at http://dx.doi.org/10.1016/j.yjmcc.2014.05.009.

Disclosures

None.

References

[1] Hirt MN, Hansen A, Eschenhagen T. Cardiac tissue engineering: state of the art. Circ Res 2014;114:354–67.
[2] Zimmermann WH, Schneiderbanger K, Schubert P, Didie M, Munzel F, Heubach JF, et al. Tissue engineering of a differentiated cardiac muscle construct. Circ Res 2002;90:223–30.
[3] Hansen A, Eder A, Bonstrup M, Flato M, Mewe M, Schaaf S, et al. Development of a drug screening platform based on engineered heart tissue. Circ Res 2010;107:35–44.
[4] Schaaf S, Shibamiya A, Mewe M, Eder A, Stohr A, Hirt MN, et al. Human engineered heart tissue as a versatile tool in basic research and preclinical toxicology. PLoS One 2011;6:e26397.
[5] Radisic M, Park H, Shing H, Consi T, Schoen FJ, Langer R, et al. Functional assembly of engineered myocardium by electrical stimulation of cardiac myocytes cultured on scaffolds. Proc Natl Acad Sci U S A 2004;101:18129–34.
[6] Tulloch NL, Muskheli V, Razumova MV, Korte FS, Regnier M, Hauch KD, et al. Growth of engineered human myocardium with mechanical loading and vascular coculture. Circ Res 2011;109:47–59.
[7] Jacobson SL, Piper HM. Cell cultures of adult cardiomyocytes as models of the myocardium. J Mol Cell Cardiol 1986;18:661–78.
[8] van der Velden J, Klein LJ, van der Bijl M, Huybregts MA, Stooker W, Witkop J, et al. Force production in mechanically isolated cardiac myocytes from human ventricular muscle tissue. Cardiovasc Res 1998;38:414–23.
[9] Eschenhagen T, Eder A, Vollert I, Hansen A. Physiological aspects of cardiac tissue engineering. Am J Physiol Heart Circ Physiol 2012;303:H133–43.
[10] Zhang D, Shadrin IY, Lam J, Xian HQ, Snodgrass HR, Bursac N. Tissue-engineered cardiac patch for advanced functional maturation of human ESC-derived cardiomyocytes. Biomaterials 2013;34:5813–20.
[11] Hirt MN, Sorensen NA, Bartholdt LM, Boeddinghaus J, Schaaf S, Eder A, et al. Increased afterload induces pathological cardiac hypertrophy: a new in vitro model. Basic Res Cardiol 2012;107:307.
[12] Stoehr A, Neuber C, Baldauf C, Vollert I, Friedrich FW, Flenner F, et al. Automated analysis of contractile force and Ca2+ transients in engineered heart tissue. Am J Physiol Heart Circ Physiol 2014 May;306(9):H1353–63. http://dx.doi.org/10.1152/ajpheart.00705.2013.
[13] Harding SE, Vescovo G, Kirby M, Jones SM, Gurden J, Poole-Wilson PA. Contractile responses of isolated adult rat and rabbit cardiac myocytes to isoproterenol and calcium. J Mol Cell Cardiol 1988;20:635–47.
[14] Cain BS, Meldrum DR, Meng X, Shames BD, Banerjee A, Harken AH. Calcium preconditioning in human myocardium. Ann Thorac Surg 1998;65:1065–70.
[15] Tiburcy M, Didie M, Boy O, Christalla P, Doker S, Naito H, et al. Terminal differentiation, advanced organotypic maturation, and modeling of hypertrophic growth in engineered heart tissue. Circ Res 2011;109:1105–14.
[16] Zeng QC, Guo Y, Liu L, Zhang XZ, Li RX, Zhang CQ, et al. Cardiac fibroblast-derived extracellular matrix produced in vitro stimulates growth and metabolism of cultured ventricular cells. Int Heart J 2013;54:40–4.
[17] Naito H, Melnychenko I, Didie M, Schneiderbanger K, Schubert P, Rosenkranz S, et al. Optimizing engineered heart tissue for therapeutic applications as surrogate heart muscle. Circulation 2006;114:I72–8.
[18] Zhu WZ, Xie Y, Moyes KW, Gold JD, Askari B, Laflamme MA. Neuregulin/ErbB signaling regulates cardiac subtype specification in differentiating human embryonic stem cells. Circ Res 2010;107:776–86.
[19] McMullen JR, Shioi T, Huang WY, Zhang L, Tarnavski O, Bisping E, et al. The insulin-like growth factor 1 receptor induces physiological heart growth via the phosphoinositide 3-kinase(p110alpha) pathway. J Biol Chem 2004;279:4782–93.
[20] Carrier RL, Rupnick M, Langer R, Schoen FJ, Freed LE, Vunjak-Novakovic G. Effects of oxygen on engineered cardiac muscle. Biotechnol Bioeng 2002;78:617–25.
[21] Zimmermann WH, Melnychenko I, Wasmeier G, Didie M, Naito H, Nixdorff U, et al. Engineered heart tissue grafts improve systolic and diastolic function in infarcted rat hearts. Nat Med 2006;12:452–8.
[22] Nuccitelli R. Endogenous ionic currents and DC electric fields in multicellular animal tissues. Bioelectromagnetics 1992(Suppl. 1):147–57.
[23] Lasher RA, Pahnke AQ, Johnson JM, Sachse FB, Hitchcock RW. Electrical stimulation directs engineered cardiac tissue to an age-matched native phenotype. J Tissue Eng 2012;3 [2041731412455354].
[24] Moretti A, Bellin M, Welling A, Jung CB, Lam JT, Bott-Flugel L, et al. Patient-specific induced pluripotent stem-cell models for long-QT syndrome. N Engl J Med 2010;363:1397–409.
[25] Tohyama S, Hattori F, Sano M, Hishiki T, Nagahata Y, Matsuura T, et al. Distinct metabolic flow enables large-scale purification of mouse and human pluripotent stem cell-derived cardiomyocytes. Cell Stem Cell 2013;12:127–37.
[26] Bullough DA, Potter S, Fox MH, Zhang C, Metzner EK, Mullane KM. Acadesine prevents oxidant-induced damage in the isolated guinea pig heart. J Pharmacol Exp Ther 1993;266:666–72.
[27] Feletou M, Vanhoutte PM. Relaxation of canine coronary artery to electrical stimulation: limited role of free radicals. Am J Physiol 1987;253:H884–9.
[28] Lamb FS, Webb RC. Vascular effects of free radicals generated by electrical stimulation. Am J Physiol 1984;247:H709–14.
[29] Tandon N, Marsano A, Maidhof R, Wan L, Park H, Vunjak-Novakovic G. Optimization of electrical stimulation parameters for cardiac tissue engineering. J Tissue Eng Regen Med 2011;5:e115–25.
[30] Luther PK. Three-dimensional structure of a vertebrate muscle Z-band: implications for titin and alpha-actinin binding. J Struct Biol 2000;129:1–16.
[31] Berger HJ, Prasad SK, Davidoff AJ, Pimental D, Ellingsen O, Marsh JD, et al. Continual electric field stimulation preserves contractile function of adult ventricular myocytes in primary culture. Am J Physiol 1994;266:H341–9.
[32] Nunes SS, Miklas JW, Liu J, Aschar-Sobbi R, Xiao Y, Zhang B, et al. Biowire: a platform for maturation of human pluripotent stem cell-derived cardiomyocytes. Nat Methods 2013;10:781–7.
[33] Tandon N, Cannizzaro C, Chao PH, Maidhof R, Marsano A, Au HT, et al. Electrical stimulation systems for cardiac tissue engineering. Nat Protoc 2009;4:155–73.
[34] Thavandiran N, Dubois N, Mikryukov A, Masse S, Beca B, Simmons CA, et al. Design and formulation of functional pluripotent stem cell-derived cardiac microtissues. Proc Natl Acad Sci U S A 2013;110:E4698–707.
[35] Tong CW, De Lange WJ, Ralphe JC. Pacing during culture improves performance of engineered cardiac tissue. Abstracts from the 2009 Annual Meeting of the International Society for Heart Research North American Section, P-55. Baltimore, Maryland, USA. J Mol Cell Cardiol 2009:S1–S55.
[36] Dhillon PS, Gray R, Kojodjojo P, Jabr R, Chowdhury R, Fry CH, et al. Relationship between gap-junctional conductance and conduction velocity in Mammalian myocardium. Circ Arrhythm Electrophysiol 2013;6:1208–14.

[37] Bers DM, Despa S, Bossuyt J. Regulation of Ca2 + and Na + in normal and failing cardiac myocytes. Ann N Y Acad Sci 2006;1080:165–77.
[38] Barbuti A, Baruscotti M, DiFrancesco D. The pacemaker current: from basics to the clinics. J Cardiovasc Electrophysiol 2007;18:342–7.
[39] Hikoso S, Yamaguchi O, Nakano Y, Takeda T, Omiya S, Mizote I, et al. The I{kappa}B kinase {beta}/nuclear factor {kappa}B signaling pathway protects the heart from hemodynamic stress mediated by the regulation of manganese superoxide dismutase expression. Circ Res 2009;105:70–9.